Hydrological Sciences Journal

ISSN: (Print) (Online) Journal homepage: https://www.tandfonline.com/loi/thsj20

The role of urbanization in the flooding and surface water chemistry of Puerto Rico's mangroves

Benjamin L. Branoff

To cite this article: Benjamin L. Branoff (2020) The role of urbanization in the flooding and surface water chemistry of Puerto Rico's mangroves, Hydrological Sciences Journal, 65:8, 1326-1343, DOI: 10.1080/02626667.2020.1747620

To link to this article: https://doi.org/10.1080/02626667.2020.1747620

HYDROLOGICAL SCIENCES JOURNAL
2020, VOL. 65, NO. 8, 1326–1343
https://doi.org/10.1080/02626667.2020.1747620

The role of urbanization in the flooding and surface water chemistry of Puerto Rico's mangroves

Benjamin L. Branoff

Gulf Ecosystem Measurement and Modeling Division, Office of Research and Development, United States Environmental Protection Agency, Gulf Breeze, FL, USA

ABSTRACT

In this study, water level models are constructed to characterize mangrove flooding across urban gradients in Puerto Rico. The most urban sites exhibited 95% longer hydroperiods, 23% lower flood frequencies, and 110% lower depths than the least urban sites. Rainfall importance was explained more by geomorphology and tidal connectivity than by urbanization, but there was evidence for changes in tidal amplitudes along the urban gradient. Relationships between surface water chemical metrics and land cover contradicted previous studies by suggesting lower nutrients and biochemical oxygen demand with increasing urbanization. However, much of this changed with the exclusion of potential outlier sites, as well as under different statistical comparisons. These results reinforce the understanding that the most important drivers of urban mangrove hydrology and water quality in Puerto Rico are likely geomorphology and tidal connectivity, with some influence from surrounding land cover. Results should be considered alongside the reported errors stemming from digital elevation and rainfall response models.

ARTICLE HISTORY
Received 17 April 2019
Accepted 11 February 2020

EDITOR
Archfield

ASSOCIATE EDITOR
R. van Nooijen

KEYWORDS
urban mangroves; Anthropocene; novel ecosystems; storm water; tidal harmonics; flooding

Introduction

As forested tidal wetlands along primarily tropical and subtropical coastlines, mangroves are often under pressure from urban development and the subsequent effects on surface water chemistry and hydrology, both of which play important roles in ecosystem function and the provisioning of services (Lugo and Snedaker 1974, Wolanski *et al.* 1993, Ewel *et al.* 1998, Medina 1999, Bosire *et al.* 2008, Lee *et al.* 2014). Specifically, metrics of flooding frequency, duration, and depth have been singled out as most important in influencing mangrove physiology and zonation (Krauss *et al.* 2006, Bosire *et al.* 2008, Lugo and Medina 2014). Likewise, concentrations of nitrogen and phosphorus as well as salinity and temperature have also been shown to be important indicators of mangrove nutrition, stress, and function (Medina 1999, Feller *et al.* 2003, Lovelock *et al.* 2009). Tides and rainfall contribute to system hydrology and water chemistry (Twilley and Chen 1998, Sutula *et al.* 2001), but groundwater, fluvial, and anthropogenic contributions may also be important in some systems (Ellison and Farnsworth 1996, Lee *et al.* 2006, Sakho *et al.* 2011, Gleeson *et al.* 2013). Variations in geomorphology, which influence the breadth of the above hydrological contributions, are another important consideration when assessing mangrove ecosystems (Kjerfve *et al.* 1999, Adame *et al.* 2010). The complexity of this suite of potential influences is likely exacerbated in highly urban systems, where surface water flow and chemistry are directly and indirectly altered through impervious surfaces, infrastructure, and engineering projects (Leopold 1968, Hollis 1975, Mcclelland and Valiela 1998, Lee *et al.* 2006, Dietz and Clausen 2008). Although urban mangrove hydrology has been shown to be abnormal in some cases, few studies identify or quantify the specific influence of urbanization on hydrology or surface water chemistry.

Lee *et al.* (2006) argue that the primary influence of urbanization on coastal wetlands is either directly or indirectly a result of changes to hydrology and sedimentation, which vary spatially and temporally in intensity. This is corroborated for forested wetlands in general (Faulkner 2004), but mangroves are unique in their tidal connectivity and specific examples from urban systems are scarce. A number of studies point to changes in mangrove coverage following large engineering projects that alter surrounding geomorphology, but these are not necessarily related to urbanization, or use qualitative or otherwise ambiguous definitions of "urban" (Colonnello and Medina 1998, Tian-Hong *et al.* 2008, Sakho *et al.* 2011, Marois and Mitsch 2017). As for water quality, it is widely shown that, relative to forested or un-populated and non-agricultural areas, urban watersheds are characterized by higher nitrogen fluxes and retention (Groffman *et al.* 2004, Yang 2012, Wigand *et al.* 2014), which may lead to higher oxygen demand and lower dissolved oxygen (House *et al.* 1993, Pagliosa *et al.* 2006, Villate *et al.* 2013). But many nutrients and especially nitrogen are non-conservative and subject to repeated and rapid biotransformation, especially in tidally flushed mangrove estuaries (Singh *et al.* 2005, Reef *et al.* 2010). Thus, elevated nitrogen concentrations in urban mangroves may not necessarily be due to anthropogenic influences. Still, the influence of municipal sewage discharge on mangroves has been well documented and associated with nutrient enrichment, heavy metal contamination, and sometimes mortality (Clough *et al.* 1983, Mandura 1997, Wong *et al.* 1997, Branoff 2017). Yet few

CONTACT Benjamin L. Branoff branoff.benjamin@epa.gov Gulf Ecosystem Measurement and Modeling Division, Office of Research and Development, United States Environmental Protection Agency, Gulf Breeze, FL, USA

studies directly link quantified variations in urbanization metrics, such as impervious surface coverage, population density, or forested area, with changes in mangrove flooding dynamics or surface water chemistry.

In San Juan, Puerto Rico, the mangroves have long been associated with ecological abnormalities due to ongoing urbanization (Seguinot Barbosa 1996), but again, there remains no direct ties between the relative intensity of urbanization and changes in flooding metrics or surface water chemistry. The geomorphology of the San Juan Bay Estuary has been modified through canalization or dredging or both over the course of the city's 500 year history (Ellis 1976, Cerco *et al.* 2003). This has resulted in changes in underlying aquifer levels and salinities, as well as surface water chemistry and connectivity that are often associated with risks to both human and ecological health (Seguinot Barbosa 1996, Bunch *et al.* 2000). Large-scale engineering projects have since been proposed to mitigate these issues (Cerco *et al.* 2003), and are currently in various phases of implementation. However, apart from sewage discharge, there has been no reported effort to understand how specific components of the urban landscape (e.g. impervious surfaces, roads, population density) may be influencing mangrove flooding metrics or surface water chemistry. This holds true for the various other coastal urban watersheds of Puerto Rico, where mangroves have endured a long history of anthropogenic influences (Martinuzzi *et al.* 2009).

This study aims to characterize and model surface water fluctuations in the mangroves of three watersheds in Puerto Rico, using both long and short-term water level recordings, as well as rainfall and tidal harmonics models. It then uses these models alongside digital elevation models to analyze the flooding dynamics of the mangroves and correlates these, as well as surface water chemical properties, with surrounding land cover along gradients of urbanization. Specifically, this study tests the hypothesis that increasing surrounding urbanization is associated with variations in mangrove flooding and surface water chemistry. These connections must be well-understood for successful mangrove management (Lewis 2005, Bosire *et al.* 2008), and will be important in understanding the influence of urban land cover on mangrove ecology, especially in the context of future floral and faunal censuses in the study areas.

Methods

Three watersheds in Puerto Rico were selected based on the range in urbanization surrounding their mangroves. This was calculated as described below using spatial datasets of urban, open water, and vegetation classifications, as well as mangrove extent, population density and road lengths. These were combined as an urban index value to give a single relative representation of urbanization for one hundred random mangrove locations in all watersheds of Puerto Rico (Fig. 1(a) and (b)). The urban index is a combination of urban land use, vegetation and open water coverage, population density, and road length. Sites were selected within three watersheds to give the greatest possible range in urbanization within the mangroves (Fig. 1(c)). Water chemistry measurements were only available for the San Juan Bay Estuary.

Study locations

Three watersheds were chosen because their mangroves held the greatest range of urbanization. They are the San Juan Bay Estuary, the Río Inabón to the Río Loco (Ponce), and the Río de la Plata (Levittown) (Fig. 1(a)). The San Juan Bay estuary was divided into 10 separate mangrove regions, and Ponce and Levittown into three regions each. This resulted in 16 study locations throughout the three watersheds.

The San Juan metropolitan area lies within the watershed described as between the Río Grande de Loíza and the Río Bayamon. The 240-km^2 drainage basin encompasses 25 km^2 of open water, consisting of five embayments connected by a system of natural and canalized channels (Bunch *et al.* 2000). The estuary is home to the island's largest and densest human population, 0.5 million people and 1800 people/km^2 in the municipalities of San Juan, Carolina and Bayamón (USCB 2017a). Given the intense human presence around the estuary, a number of studies have described its hydrodynamic and contamination issues, which range from eutrophication and heavy metals to tidal flushing and connectivity (Webb and Gómez-Gómez 1998, Bunch *et al.* 2000, Cerco *et al.* 2003, Acevedo-Figueroa *et al.* 2006). The estuary also harbors the islands largest mangrove forest, Bosque Estatal de Piñones, which at 2550 ha represents roughly 11% of the watershed area (Brandeis *et al.* 2014). The combination of intense urbanization and expansive forested and open water areas within this watershed results in the greatest range in mangrove urbanization on the island. The median (more "typical") annual rainfall for this site was 1585 ± 642 mm from 2012 to 2017 (this study).

Dredging and canalization have occurred throughout the estuary and continue to be proposed (Ellis 1976, Seguinot-Barbosa 1983, USACE 2015). Previous dredging has taken place in the San Juan Bay, and the Condado, San Jose and Torrecilla lagoons from the 1950s to the 1970s (Ellis 1976). These projects increased lagoon volumes and flow rates through canals, and decreased surface areas where dredging material was placed along shorelines. It is expected that this has resulted in lower residence times for sewage effluents and storm-water discharge, but greater prevalence of anaerobic zones.

Levittown refers to the mangroves associated with the town of Levittown, in Toa Baja, Puerto Rico, which falls within the Río de la Plata watershed, just west of the San Juan Bay Estuary. The estuary is composed of an artificial tidal lagoon constructed to drain surrounding settlements and connected to the ocean through a tidal creek and permanent inlet. Little is reported on these mangroves, although the estuary has been the focus of flood mitigation efforts for surrounding neighborhoods (USACE 1987). One informal water quality survey suggested elevated sewage input as evident in high fecal coliform loads and high nutrient concentrations, as well as minimal tidal connectivity and the temporary influence of precipitation on water levels and salinity (USCB 2017b). Levittown median annual rainfall from 2012 to 2017 was 1752 ± 260 mm (this study).

The island's second largest metropolitan area is Ponce, which falls within the watershed described as lying between the Río Inabón and the Río Loco on the southern Caribbean

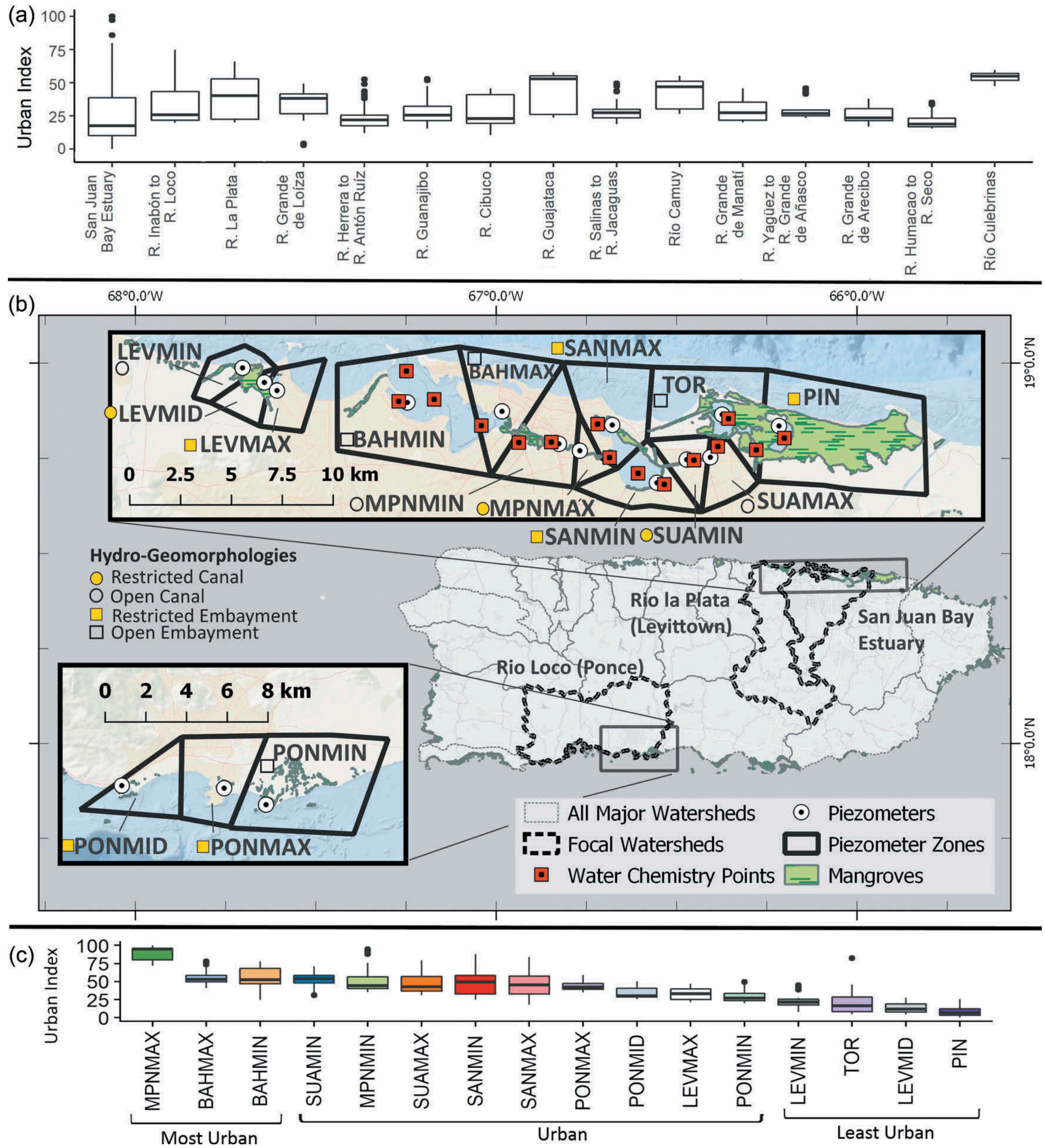

Figure 1. (a) Watersheds ordered form left to right in decreasing urbanization range. (b) Map of the study area showing location of piezometers within the selected watersheds, and (c) gradient of urbanization across all sites. Inlay polygons: individual piezometer zones. BAH: San Juan Bay, MPN: Caño Martín Peña, SAN: San José lagoon, SUA: Suarez Canal, TOR: Torrecilla Lagoon, PIN: Piñones Lagoon, LEV: Levittown and PON: Ponce. "MAX" and "MIN" in the location names refer to urbanization levels within each zone. "Most Urban", "Urban", and "Least Urban" are defined by the quantiles of the urban index.

coast. Unlike the other two watersheds, the mangrove sites at Ponce are largely unconnected and do not share the same estuarine conditions. The three mangrove forests within this study were located at Punta Cabullones, the Rafael Cordero Santiago Port of the Americas, and on the northern shore of Laguna de Salinas at Punta Cucharas. One study has covered the hydrology and water quality of some of these mangroves (Rodríguez-Martínez and Soler-López 2014), which found dissolved oxygen, specific conductance, and salinity to be dependent upon seasonal changes in hydrologic inputs during the wet and dry seasons. The site received a median annual rainfall of 869 ± 83 mm from 2012 to 2017 (this study).

Based on aerial imagery and previously mentioned hydrological studies, sites have been classified into hydrogeomorphic settings of embayments (i.e. ocean, bay, or lagoon) or canals, and either open or partially restricted to tidal exchange (Fig. 1(b)). Ocean and bay sites by their nature have direct tidal exchange and are thus always classified as open. These sites are the two San Juan Bay sites BAHMIN and BAHMAX, and the ocean site in Ponce, PONMIN. Lagoon or canal sites may have open or partial tidal exchange. Torrecilla lagoon is an open lagoon due to its dredged mouth at Boca de Cangrejos (Ellis 1976). Open canals are the east end of Suárez canal, SUAMAX, which shares the dredged connection with Torrecilla, the west and dredged portion of the Caño Martin Peña, MPNMIN, and the mouth of the Río Cocal in Levittown, LEVMIN. In contrast, partially restricted canals are that connecting the Río Cocal to the Levittown lakes, LEVMID, and the undredged eastern portion of the Caño Martín Peña, MPNMAX. Partially restricted embayments are those of Piñones (PIN) and San José (SANMIN and SANMAX) in the San Juan Bay Estuary, Levittown lakes (LEVMAX) in Levittown, and the Salinas lagoon (PONMID) and the Port of the Americas in Ponce (PONMAX).

Calculating urbanization

Spatial datasets used for the selection of study sites and the calculation of urban variables are described in Table 1. All spatial analyses and modeling was performed in the R programming language (Yan *et al.* 2011). Individual functions in R are stated along with their corresponding packages and authors. Packages used in these analyses include *sp* (Bivand *et al.* 2013), *rgeos* (Bivand and Rundel 2017), and *raster* (Hijmans 2016). A schematic outlining the process is presented in Fig. 2.

To begin, 100 random points were placed within mangrove classified habitat in each watershed of Puerto Rico (NOAA BP 2011). To assess the surrounding land coverage, a sampling circle of radius 500 m was created around each point, and mangrove coverage and land cover datasets were then cropped and masked to include only those cells within the circle. The total mangrove coverage for each point was then calculated by summing the mangrove cell values. Land cover was calculated by first counting the number of cells within each class, in which urban was classes 2 and 5 (Impervious and Developed Open Space, respectively), and green and blue area was the sum of all vegetation and open water classes, defined as classes 6–18 and 21. These sums were then multiplied by the area of each cell, which had a mean of 2.01 m^2.

Road lengths within each circle were calculated by first clipping the entire road network to include only the area within the circle and summing the combined length. Population density within the sampling circle was calculated using 2010 US Census data at the block level. The total population within the sampling circle was calculated assuming all people lived in non-road impervious surfaces. The area of non-road impervious surfaces within each block was calculated by first obtaining the total area of impervious surfaces through the methods of the previous paragraph, using the boundary of each census block to sample the land cover within. This was then used to calculate the population density per unit area of non-road impervious surfaces for each block, which was then multiplied by the area of non-road impervious surfaces within each part of each census block contained in the circular sampling area. This resulted in the total number of people within the sampling area, which was then divided by the area of the circle to give the population density.

Table 1. Spatial datasets used to determine relative elevations and to quantify the urbanization surrounding each study site. Variables were sampled from a sampling area described by a circle of radius 500 m and centered on individual study sites.

Variable	Dataset Description	Source
Land cover Urban Vegetation and water	2-m resolution land cover raster for Puerto Rico in 2010	Office for Coastal Management (2020)
Mangrove coverage	30-m resolution continuous mangrove coverage raster for 2012	Hamilton and Casey (2016)
Population density	Total population shapefile for 2010 in Puerto Rico by census block	USCB (2017a)
Road length	Road network shapefile for Puerto Rico in 2015	USCB (2017b)
Elevation	DEMs for sites, at 3- and 1-m horizontal resolution and 9- and 4.2-cm vertical accuracy for the northern and southern sites, respectively	NOAA (2017a, 2017b)

These variables were used independently in further analyses, along with a combination of all of them representing an urban index at each location. The index was calculated based upon a similar method for aquatic ecosystems (Mcmahon and Cuffney 2000). The urban index value is calculated using the following equation:

$$\text{Urban Index} = \frac{\sum_{i=0}^{n} Y_i}{n} \tag{1}$$

where n is the number of variables used in the index, in this case the five variables of urban area, green and blue area, mangrove area, populations density, and road length. Y_i represents the variables normalized to a range of 0 to 100 through the following equation:

$$Y = 100 \times (X - X_{\min}) \div (X_{\max} - X_{\min}) \tag{2}$$

in which Y and X represent the normalized and raw values, respectively. In the case of mangrove and blue-green coverage, the normalized variable was reversed by subtracting from 100, so that lower values represent a greater degree of urbanization. The urban index is thus a representation of the relative intensity of urbanization, in which 100 is the most urban site and 1 is the least urban site. Sites were also classified into categories based on their quartiles of the urban index, such that "Most Urban" sites are those with an urban index greater than the third quartile, "Least Urban" sites are those with an urban index lower than the first quartile, and "Urban" sites are those in between the first and third quartiles.

Water level and weather data acquisition

Water levels models were constructed from water level recordings made throughout the study area and from precipitation and barometric pressure observations from nearby weather stations. The models covered a 5-year period, from 1 June 2012 to 1 June 2017. Additional utilized packages not mentioned below are the zoo (Zeilis and Grothendieck 2005), RJSONIO (Temple Lang 2014), and HyetosMinute packages (Koutsoyiannis and Onof 2001).

Water levels

Water levels were recorded in 16 locations within the three watersheds in Puerto Rico (Fig. 1(b)). Piezometer wells were constructed from 2-m segments of 7.62-cm diameter PVC tubing. One half of the length of the well was perforated with 1 mm x 1 cm slits placed every 1 cm using a sanding disc attached to a Dremel rotary tool. The wells were capped with PVC caps and one Onset HOBO U20l water-level logger was hung from a 1.75-m cable attached to the top cap. Wells were placed in holes excavated at the shoreline using a 7.62-cm corer to a depth of

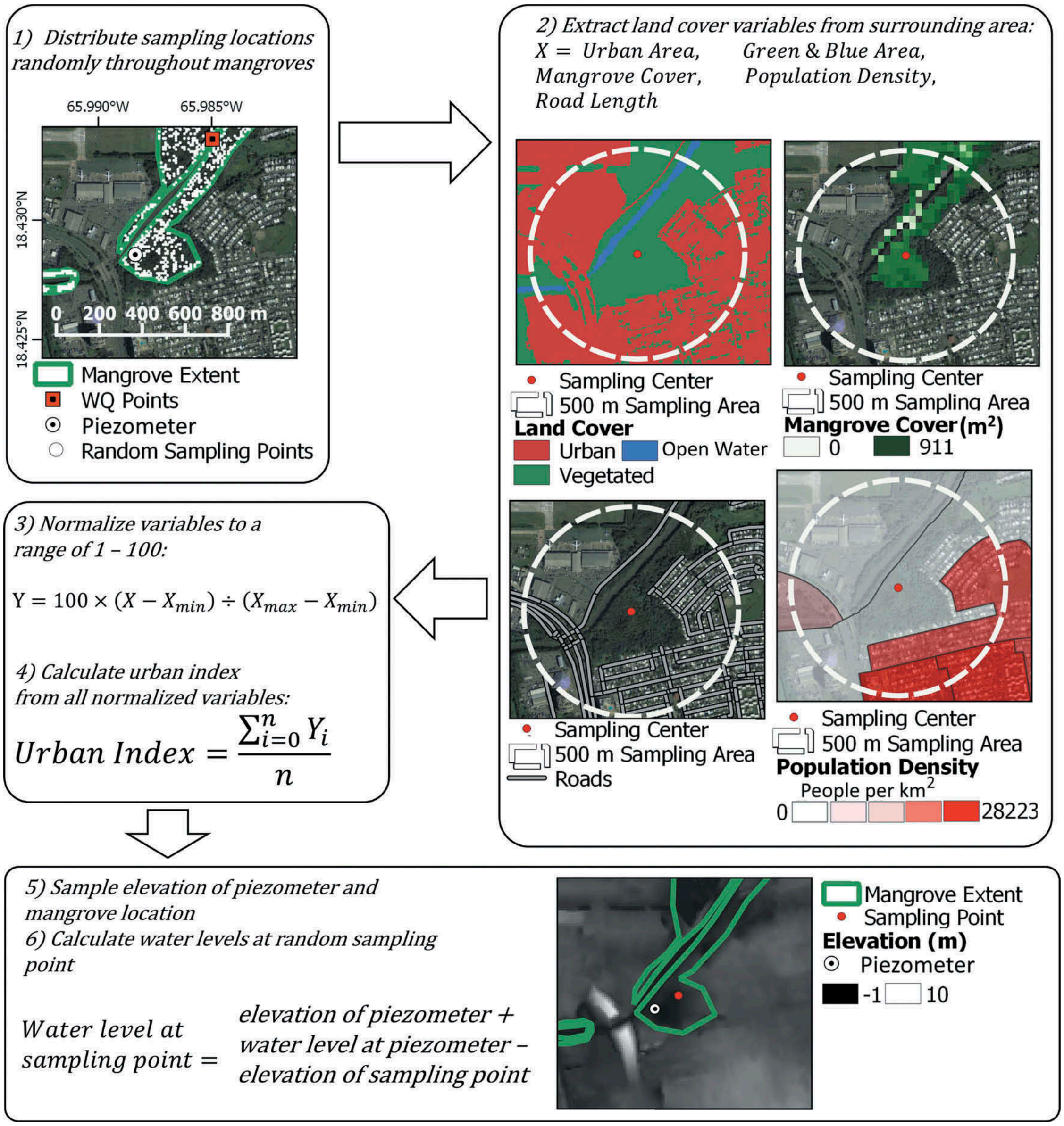

Figure 2. Schematic of the spatial sampling routine for calculating the urban index and water levels at random mangrove locations throughout the study area. Commented subroutines for these analyses are provided at github.com/BBranoff/Urban-Mangrove-Hydrology. Sampling locations were distributed randomly throughout the mangrove habitat. Land cover within the surrounding 500 m of these locations was then sampled and used to calculate the urban index. Elevations were sampled at each location and at the nearest piezometer, which were used to calculate the water levels at all locations.

1.5 m. The water-level loggers were programmed to take pressure and temperature readings every 15 min. Data were extracted using an Onset HOBO waterproof shuttle at varying intervals averaging once every three months. Water levels were calculated from pressure readings using the HOBO barometric compensation tool in the HOBO Pro software and atmospheric pressure readings recorded at varying locations as described below.

Weather data

Site precipitation and atmospheric pressure were acquired from varying sources as detailed in Table 2 and assembled into 1-hour observations over the 5-year period. Hourly observations were collected from The Weather Underground website (wunderground.com) using their Weather API feature (Table 2). For San Juan (SJU), this represented a complete set of observations, but the two other locations required additional data sources and approximations to compensate for large gaps in The Weather Underground data. Missing precipitation data were filled using daily values from the National Climate Data Center at various stations (Table 2). Hourly rainfall from these stations was reconstructed from the daily data through the *DisagSimul* function. Missing barometric pressure observations were approximated using a linear interpolation between known values calculated through the *na.approx* function.

Surface water chemical properties

Surface water chemical properties were only available for the San Juan Bay Estuary, where most of the study sites are found. Measurements were downloaded from the San Juan Bay Estuary Program's water quality monitoring program. Monthly metrics were pH, temperature (°C), dissolved oxygen (DO; mg/L), salinity (PSS), and turbidity (NTU).

Table 2. Weather data sources for the three regions included in the study (San Juan, Ponce, and Levittown, Puerto Rico). NCDC: National Climate Data Center. Percent of observations: percentage of total rain observations for each watershed that were obtained from the corresponding sources.

Data type	Location	Station ID	Source	Percent of observations
Hourly precipitation and atmospheric pressure	San Juan: 18.4365°N, – 66.0069°W	SJU	Wunderground weather station	100%
Daily precipitation	Levittown: 18.4356°N, – 66.1678°W	RQC00669415	NCDC	96%
Hourly precipitation and atmospheric pressure	Levittown: 18.4422°N, – 66.1786°W	ITOABAJA2	Wunderground Personal Weather Station	4%
Daily precipitation	Ponce: 18.0258°N, – 66.5252°W	RQC00667292	NCDC	39%
	Ponce: 18.0318°N, – 66.5996°W	RQ1PRPC0002	NCDC	27%
	Ponce: 18.0374°N, – 66.6017°W	RQ1PRPC0005	NCDC	19%
	Ponce: 18.0046°N, – 66.55891°W	RQ1PRPC0001	NCDC	10%
	Ponce: 18.0125°N, – 66.5874°W	RQ1PRPC0006	NCDC	6%
Hourly precipitation and atmospheric pressure	Ponce: 18.0086°N, – 66.5635°W	TJPS	Wunderground weather station	47%

Biannual metrics were total Kjeldahl nitrogen (mg/L), total nitrate and nitrite (mg/L), total phosphorous (mg/L), total organic carbon (TOC; mg/L), ammonium (mg/L), biological oxygen demand (BOD; mg/L), and oil and grease (mg./L). The lowest detection limits and total number of samples for each metric at each study site are presented in Table 3. Although mangrove nutrition would be more accurately represented by pore-water chemistry, there is a documented relationship between surface and pore-water in mangrove systems (Bouillon *et al.* 2007, Gleeson *et al.* 2013), and also between surface water chemistry and mangrove distribution (Sherman *et al.* 1998). Thus, these relatively easier to obtain surface water measurements will serve as a good indication of the mangrove chemical environment over a large area.

Modeling

As with all other analyses, water level modeling was done in the R programming language.[1] In addition to the packages mentioned below, the TTR (Ulrich 2017), *zoo* (Zeilis and Grothendieck 2005), *minqa* (Bates *et al.* 2014), and *relaimpo* packages (Grömping 2006) were also used throughout the process. Water levels at each location were modeled using a combination of tidal and precipitation inputs. Contributions from stream and groundwater inputs, or losses from evapotranspiration were not included as no reliable measurements were available for the study areas. Tidal components were modeled through the *ftide* function in the TideHarmonics package (Stephenson 2016), which uses timestamped water level observations to compute model coefficients for up to 409 harmonic tidal constituents. Constituent amplitudes and phases interact to give a change in water level, relative to the mean. Water levels due to tides at a given time,$\mathrm{Tides}(t)$, can thus be modeled from all N harmonic constituents by summing each individual n constituent using the following equation from Stephenson (2016):

$$\mathrm{Tides}(t) = \sum\nolimits_{n=1}^{N} f_n A_n \cos\left(\frac{\pi}{180}\left(\omega_n t + u_n + V_n - \psi_n\right)\right) \quad (3)$$

The amplitude, angular frequency, equilibrium phase, phase lag, and nodal corrections for each constituent are given by A_n,ω_n,V_n, ψ_n, u_n and f_n respectively. The time (t) is represented as the length, in minutes, from the origin of the model, which is dependent upon the period of observations at each site. Models were calculated for all observations in which the 4-day cumulative rainfall was less than 1 mm to avoid interference from precipitation inputs. The resulting coefficients of each tidal constituent were saved for further analyses. These models were then used with the *predict.tide* function to predict water levels every hour over the 5-year period. The result is water-level predictions based only on tidal components.

Tidal predictions were then used along with rainfall data and the observed water levels to compute contributions from precipitation. This contribution was modeled at each location through a combination of moving averages and moving sums, as has been implemented in other studies (Dawson and Wilby 1998, Toth *et al.* 2000, Altunkaynak 2007). Short-term response to rainfall was modeled with an exponential moving average (EMA) of precipitation. The short-term contribution from precipitation is thus given as:

$$\mathrm{RainEMA}(t) = \begin{cases} \frac{\sum_{t=1}^{n} \mathrm{Rain}_t}{n \cdot C}, & t = n \\ \frac{\frac{2}{n+1}\mathrm{Rain}_t + \left(1 - \frac{2}{n+1}\right)\mathrm{RainEMA}_{t-1}}{C} & t > n \end{cases} \quad (4)$$

in which Rain_t is the observed precipitation at time t, n is the moving average window, and C is a dampening constant. Long-term precipitation input was modeled using a moving sum of rainfall data in the form:

$$\mathrm{RainMS}(t) = \min + \frac{\sum_{t=1}^{n} \mathrm{Rain}_t}{C} \quad (5)$$

[1]A detailed, commented copy of the code can be found at github.com/BBranoff/Urban-Mangrove-Hydrology.

Table 3. Lowest detection limits (LDL) and sample sizes for surface water chemistry measurements taken from the San Juan Bay Estuary Program corresponding to the study period: 1 June 2012–1 June 2017. There is no station for the MPNMAX study site or for those outside of the San Juan Bay Estuary.

		San Juan Bay Estuary Program station								
		Peninsula la Esperanza Bahía de San Juan 1, Bahía de San Juan 2	Bahía de San Juan 3	Río Puerto Nuevo, Caño Martín Peña	Laguna Los Corozos, Laguna San José 1	Laguna San José 2, Quebrada San Antón	Canal Suárez 1	Canal Suárez 2	Laguna Torrecilla 2, Laguna Torrecilla 3	Laguna Piñones
Metric	LDL	BAHMIN	BAHMAX	MPNMIN	SANMAX	SANMIN	SUAMIN	SUAMAX	TOR	PIN
Ammonium (mg/L)	0.1	12	6	17	14	14	9	10	11	5
Biological oxygen demand (mg/L)	2	17	9	18	13	14	9	8	14	5
Dissolved oxygen (mg/L)	0	119	58	112	86	88	61	61	90	31
Oil & Grease (mg/L)	1.4	9	5	14	6	9	6	6	8	5
pH	2	119	59	114	86	87	61	61	90	31
Phosphorus (mg/L)	0.01	8	5	10	4	10	5	5	6	4
Salinity (PSS)		107	58	112	66	78	61	61	77	19
Temperature (°C)	−5	119	59	114	85	88	61	61	90	31
Total Kjeldahl Nitrogen (mg/L)	0.2	9	5	17	15	16	10	10	11	6
Total nitrite & nitrate (mg/L)	0.01	19	9	19	15	17	10	11	14	6
Total organic carbon (mg/L)	0.05	19	9	17	16	16	10	10	15	7
Turbidity (NTU)	0.05	129	61	11	87	95	60	62	97	32

in which min is the baseline water level, taken to be the minimum recorded observation, Rain is the observed precipitation in mm, n is the moving sum window, and C is a dampening constant. Coefficients for both short and long term rainfall contributions were optimized for each location using a BOBYQA optimization, by minimizing the residual sum of squares between the observed water levels and the sum of the tidal and rain models (Powell 2009).

Using the above equations, the water level at each location at any given time can be predicted by combining the tidal and precipitation components through the equation:

$$y(t) = \mathrm{Tides}(t) + \mathrm{RainEMA}(t) + \mathrm{RainMS}(t). \qquad (6)$$

In some cases, optimization resulted in zero contribution from tidal, or short and long-term rainfall contributions.

With both the tidal and precipitation contributions to water levels modeled for each piezometer, their relative importance of each in the overall model was also calculated. This was done for individual tidal constituents and for the combined rainfall constituent. Relative importance was calculated as the contribution of each constituent to the R^2 of the full model against the observations (Lindeman 1980). This importance value was calculated for the 10 tidal constituents with the greatest amplitude. The individual and cumulative R^2 of all constituents in the water level models are reported in the results.

Mangrove elevations

The above water-level models were used to predict water levels throughout the mangroves in the three watersheds of the study. This was accomplished by assuming a planar, not curved water surface from tidal asymmetry (Wolanski *et al.* 1993). Water levels at random points were calculated by subtracting their elevation from that of the observation piezometers and applying this adjustment to the predicted water levels (Fig. 2). Mangroves were defined by a benthic habitat map of Puerto Rico (National Oceanic and Atmospheric Administration Biogeography Program 2011), and elevation was taken from two 3-m horizontal resolution coastal digital elevation models (DEM), one for San Juan and Levittown (NOAA 2017b), and another for Ponce (NOAA 2017a). As with other analyses, a copy of the R subroutines is provided on GitHub.[2] Additional packages utilized but not mentioned below are *deldir* (Turner 2017), *sp* (Bivand *et al.* 2013), and *raster* (Hijmans 2016).

One thousand random points were generated within each of the 16 mangrove zones (Fig. 1(b)), and their elevations extracted from the DEMs. There were occasional small discrepancies between the benthic habitat map and the DEMs, resulting in extreme and likely mistaken elevations assigned to mangrove habitat. To remove these extreme values, the randomly sampled points were limited to elevations between the 10% and 90% quantiles. The resulting elevations were subtracted from that at the piezometer location, and this adjustment was added to the predicted water levels to give a time series of water levels at each point at every hour within the 5-year period.

Calibration and validation

Models were calibrated using the above described equations and optimization techniques on the first 90% of observations, withholding the last 10% for validation. The optimized models

[2]github.com/BBranoff/Urban-Mangrove-Hydrology.

were then validated by predicting water levels for the remaining 10% and comparing to the observations. A number of metrics were then calculated on the validation data to demonstrate the performance satisfaction of each model (Biondi *et al.* 2012, Williams and Esteves 2017). These performance criteria include the root mean square error (E_{RMS}) <0.2 m, the bias <0.2, and the Pearson correlation coefficient (cor) >0.95. The coefficient of determination (R^2) >0.5 was also used as a criterion because it infers that at least 50% of the water level variation is explained by the models. This is important in comparing the relative importance of influences on the models across sites. Because the models presented here are not intended to be used for engineering or design input, but rather for comparative ecological studies, performance criteria of $R^2 > 0.5$ and $E_{RMS} < 0.2$ m were implemented to include models in hypothesis testing. This allowed for the relative comparison of each model by ensuring that at least 50% of the water level variability was explained, while also ensuring the mean error was less than 20 cm. Hydrographs of observed and predicted water levels were also inspected to ensure satisfactory agreement. Models not meeting these criteria in both calibration and validation periods are thus reported on but excluded from hypothesis testing.

Flooding parameters

The resulting time series of water levels were analyzed for daily flooding parameters of mean flood duration, mean dry duration, mean daily flood frequency, average depth, and percent of time flooded. The same parameters were calculated for each month in the time series to correspond to monthly water quality measurements. Water levels were separated into flood (≥0) and dry (<0) conditions, and analyzed for length (hours), frequency, and mean at the daily and monthly level.

Statistical tests

Differences in predictor variables of flooding dynamics and water quality metrics between mangrove zones were identified through analysis of variance (ANOVA) using the *aov* function, and subsequent *post-hoc* differences through a Tukey honest significance test by the *TukeyHSD* function, both from base R (Yan *et al.* 2011). In testing mean differences between most urban, urban, and non urban sites, defined by the urban index (Fig. 1), the Student t-test was used through the *t.test* function of base R. Linear models were constructed through the *lm* function in base R using the form $y \sim x$ and $y \sim \log(x)$. The results were plotted using the *ggplot* function from the ggplot2 package and linear and logarithmic models through the *stat_smooth* function (Wickham 2009).

Results

Model accuracy and constituent importance

Water level model fits varied across the systems (Figs. 3 and 4). For the calibration period, all models explain 50% or more of the variation in observed water levels (R^2) and eight (57%) of the models explain 70% or more of the variation in water levels (Figs. 3(b) and 4(b)). Root mean square error (E_{RMS}) among all models during the calibration period was 7.4 cm (Figs. 3(b) and 4(b)). Validations for all models performed marginally worse than calibrations, with only 12 of the models explaining 50% or more of the variation in water levels, and a mean absolute error of 4.4 cm (Figs. 3(c) and 4(c)). Two models, LEVMAX and PONMAX, did not meet the criteria set for satisfactory agreement with observations in both calibration and validation periods ($R^2 > 0.5$, $E_{RMS} < 0.2$). These sites are thus reported on in figures as faded symbols and are excluded from further hypotheses testing involving flooding dynamics.

Constituent influences on the water levels varied in importance across the studied systems (Fig. 5). The following percentages represent the contributions of each constituent, or group of constituents, to the observed variations in water levels. In the northern sites of the San Juan Bay Estuary and in Levittown, the three most important constituents were the principal lunar semidiurnal (M2) and two lunar diurnals (K1 and O1). However, 53% and 54% of the water level variations in Piñones (PIN) and San José Lagoons (SAN), respectively, were explained by the short- and long-term precipitation models and the water levels at PIN could not be modeled using tidal constituents. In contrast, in the San Juan Bay (BAHMIN and BAHMAX) and in the dredged portion of the Caño Martin Peña (MPNMIN), precipitation explained less than 1% of the variation in water levels. In Levittown, the K1, M2 and O1 constituents combined and along with rainfall explained 45% and 54% of the variation in water levels at LEVMIN and LEVMID, respectively. Most of the remaining variation in water levels at these two sites is explained by the luni-solar synodic fortnight (Msf) and the luni-monthly (Mm). In this case, 58% of the variations in the LEVMAX station were explained only by precipitation and no tidal model could be constructed. At Ponce, the three most important constituents were the two solar diurnals (S1 and P1) and rain. These constituents explained 27%, 57%, and 31% of the water level variations at PONMIN, PONMID, and PONMAX, respectively. Rain explained 56% and 31% of the water level variations at PONMID and PONMAX, respectively, and less than 1% at PONMIN. Individual constituent model coefficients and importance metrics for each study site can be found at the studies repository: github.com/BBranoff/Urban-Mangrove-Hydrology.

Flooding dynamics

Random mangrove locations throughout the study sites varied in their flooding dynamics. Median average depths in San Juan, Levittown, and Ponce were – 1.4, – 6.0, and 0.08 cm, respectively, and means were significantly different among all watersheds (ANOVA; $p < 0.05$). Ponce depths were 8.9 cm greater than those at Levittown (ANOVA; $p < 0.001$), and 5.8 cm greater than those at San Juan ($p < 0.001$). San Juan depths were 3 cm higher than Levittown (ANOVA; $p < 0.05$). Median flood length in the three systems were 0.64, 0.17, and 2.3 days, respectively. San Juan mean flood length was 108 days longer than Levittown and 102 days longer than Ponce (ANOVA; $p < 0.001$). Median daily flood frequency, in which 0 is either constantly flooded or constantly dry, were 1.0, 0.7, and 1.1 respectively in San Juan, Levittown and Ponce. On average San Juan mangroves flooded 0.3 and 0.2 more times per day than in Levittown and Ponce

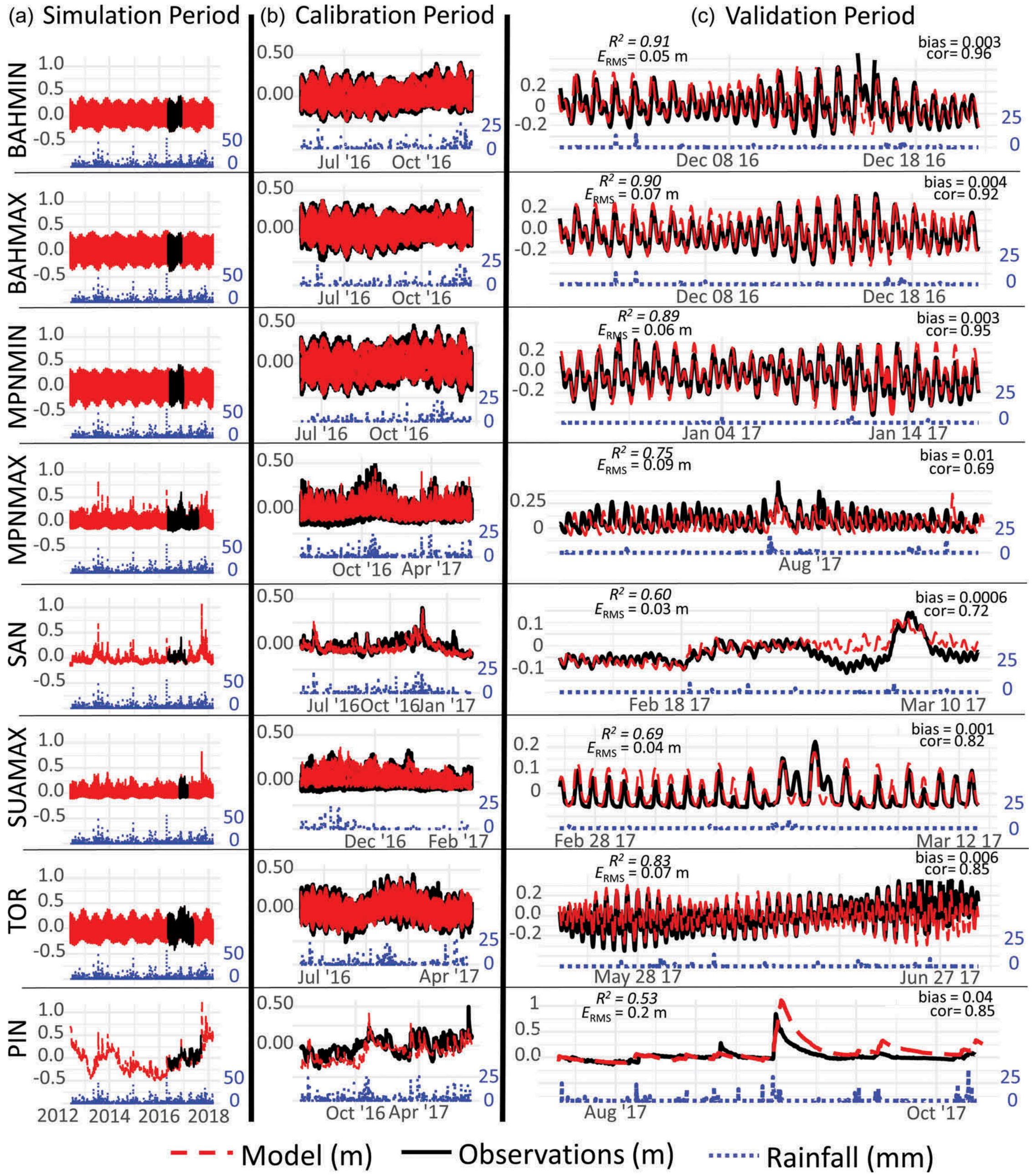

Figure 3. Rainfall, water-level observations, and water-level models in the San Juan Bay Estuary: (a) for the entire length of the analysis (2012–2017), (b) for the calibration period at each location, and (c) for the validation period. Water levels (left axis) are in reference to the mean; rainfall (right axis) is mm hr^{-1}. Water levels in (a) and (b) are on a fixed scale to highlight the difference in ranges between locations. Water-level ranges in all other panels are unique for each location. Observations and models for SANMIN, SANMAX and SUAMIN were nearly identical, and are thus here referred to as SAN.

(ANOVA; $p < 0.001$), corresponding to one extra flood every 3 and 5 days, respectively. Mangroves of Ponce flooded 0.2 times per day more than those of Levittown, corresponding to one extra flood every 5 days (ANOVA; $p < 0.01$). Median percent of time flooded was 40,11, and 48%, respectively, in San Juan, Levittown and Ponce. San Juan was flooded 13% more of the time that Levittown was flooded and 5.8% less than Ponce ($p < 0.001$). Ponce was flooded 19% more of the time than Levittown ($p < 0.001$).

Among sites, flooding metrics were variable, and no single site was distinct in all metrics. The dredged portion of Caño Martin Peña (MPNMIN) held the greatest average depth at 10 cm, which was significantly different than all other sites except Torrecilla lagoon (TORMIN) (ANOVA; mean difference: 17 cm, $p < 0.001$). In flooded depth, PONMID was greatest at 22.5 cm, which was significantly greater than all other sites except MPNMIN (ANOVA; mean difference: 12 cm, $p < 0.001$). In contrast, SANMIN experienced the lowest average depth at –24.6 cm (24.6 cm above water), which was significantly different than all sites except MPNMAX, SANMIN and SUAMIN (ANOVA; mean difference: 21 cm, $p < 0.001$).

Piñones lagoon was exceptional in hydroperiod (flood length), with a median of 20.5 days, five times longer than PONMID and at least 20 times longer than the other sites. However, SUAMAX held the greatest mean (not median) flood length at 735 days, longer than all other sites (ANOVA; mean difference: 703 days, $p < 0.001$).

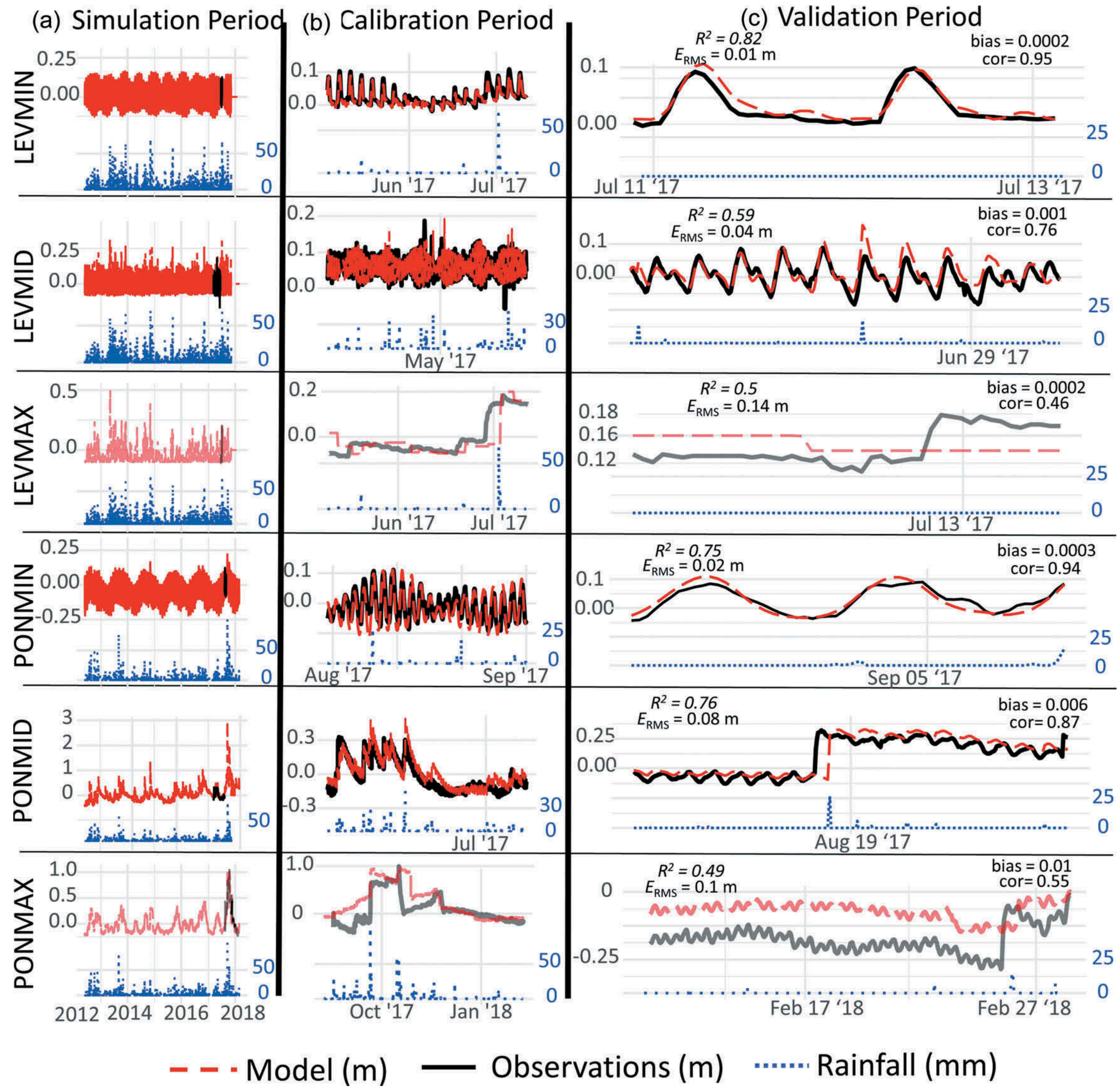

Figure 4. Rainfall, water-level observations, and water-level models in Levittown and Ponce: (a) for the entire length of the analysis (2012–2017), (b) for the calibration period at each location, and (c) for the validation period. Water levels (left axis) are in reference to the mean. Rainfall (right axis) is mm hr^{-1}. Water levels in (a) and (b) are on a fixed scale to highlight the difference in ranges between locations. Water-level ranges in all other panels are unique for each location. Models for LEVMAX and PONMAX did not meet validation criteria and are thus excluded from future hypothesis testing.

In contrast, MPNMAX exhibited the shortest hydroperiod of 0.2 days, which was lower than all other sites except LEVMID (ANOVA; mean difference: 8 days, p = < 0.001). Daily flood frequency was lowest at SANMAX at 0.2 day, which was lower than all other sites except SANMIN and SUAMIN (ANOVA; mean difference: 0.7 per day, $p < 0.001$). The highest daily flood frequency was shown by TORMIN at 2 per day, higher than all other sites (ANOVA; mean difference: 1.2 per day, $p < 0.001$). In average depth, MPNMIN was the greatest at 0.1 m and greater than all other sites (ANOVA; mean difference: 0.17 m, $p < 0.001$), and SANMAX was the least at – 0.28 m (0.28 m above water), lower than all other sites except SANMIN (ANOVA; mean difference: 0.24, $p < 0.001$).

Surface water chemical properties

In Tukey honest significant difference tests, Piñones (PIN) was singled out in surface water chemical properties. This lagoon was characterized by significantly greater total Kjeldahl nitrogen (mean difference: 8.6 mg/L; $p < 0.001$), TOC (mean difference: 12.9 mg/L; $p < 0.001$), turbidity (mean difference: 176.2 NTU; $p < 0.001$), and BOD (mean difference: 15.5 mg/L; ^ < 0.01) than all other water bodies, as well as significantly higher temperature than half of the other stations (mean difference: 1.7°C; $p < 0.05$). The BAHMAX station was also distinct in having higher salinity than all other stations (mean difference: 16.7 PSU; $p < 0.001$). SANMIN held the highest mean nitrate and nitrite concentration but was only significantly different than BAHMIN (difference: 0.3, $p < 0.05$) and SANMAX (difference: 0.3, $p < 0.05$). SANMAX held the highest pH, which was significantly different than SUAMAX (difference: 0.3, $p < 0.01$), TOR (difference: 0.3, $p < 0.01$), and PIN (difference: 0.4, $p < 0.05$). There were no differences in total phosphorus or oil and grease concentrations between sites.

Land cover, surface water chemistry and flood dynamics

Surface water chemistry metrics resulted in numerous significant models when predicted by surrounding land cover (Fig.

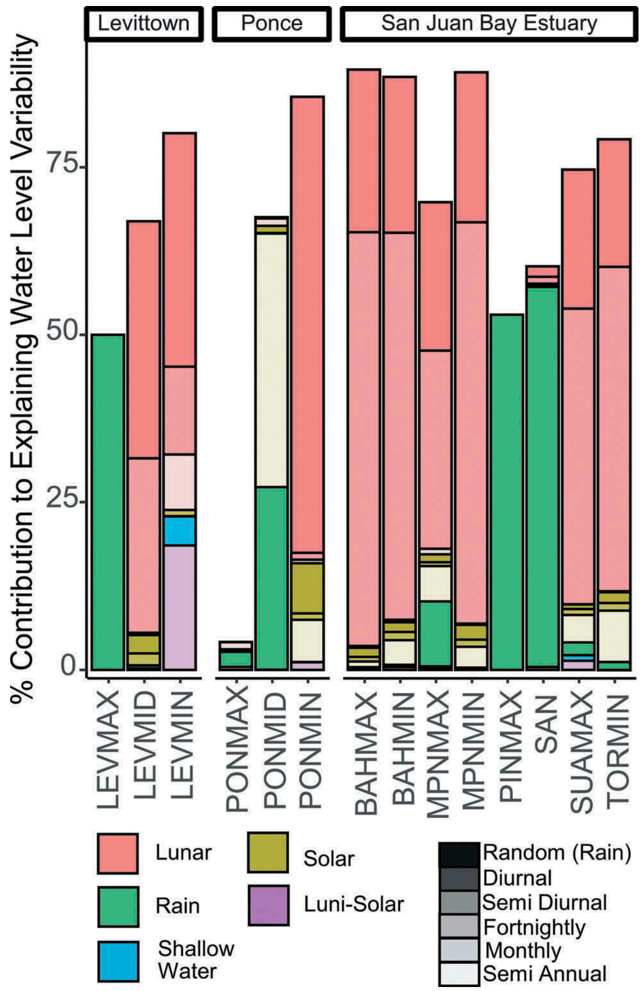

Figure 5. Mean contribution to the explained variance of the observed water levels in iterative models with varying constituent orders at each site. Lunar tidal constituents, primarily semi-diurnal, explain most of the variability at each site, except for a few lagoons with constricted tidal connectivity. Rainfall explains most of the variability at these sites, as well as some additional explanatory power from solar tidal constituents.

6). All metrics except nitrate and nitrite, total phosphorus (P), dissolved oxygen (DO), pH and salinity resulted in significant models when predicted by surrounding land cover. However, almost all models were significant only because of an outlier site, PIN (Piñones lagoon), and could not be repeated when this site was removed from the analysis. Trends suggest decreasing nitrogen, carbon, turbidity, oil, and temperature with increasing urbanization. In contrast, both Kjeldahl nitrogen ($p < 0.05$, $R^2 = 0.6$) and ammonium ($p < 0.05$, $R^2 = 0.5$) concentrations increased linearly with population density when Piñones was not considered in the analysis. When comparing the least urban sites (Piñones included) with the most urban sites (Fig. 1), nitrate and nitrite was 60% higher, while organic carbon was 60% lower and turbidity was 90% lower at the most urban sites. Likewise, salinity, temperature, and oil concentrations were 17%, 3%, and 60% lower, respectively at the most urban sites. Salinity was found to significantly increase with daily flood frequency (linear model; $R^2 = 0.55$, $p < 0.05$), and oil and grease concentrations were found to increase with flooding duration and proportion of time flooded (linear models; $R^2 = 0.5$, $p < 0.05$).

Flooding metrics resulted in fewer significant linear models compared to surface water chemical properties when predicted by surrounding land coverage (Fig. 7).

Mean water depth and the proportion of time flooded were the only flooding metrics to result in significant linear models ($p < 0.05$). In both cases, the surrounding open water and vegetation coverage was the strongest predictor and resulted in positive linear relationships. However, much of the significance of these models may only be due to the highly urban outlier site of MPNMAX, and none of the models were significant when this site was removed from the analysis. In contrast, in binomial comparisons of the most urban and least urban sites through t-tests, all metrics except the mean food depth were statistically different. These tests suggest the most urban sites have around 110% lower depths and 23% lower daily flood frequency, but 100% longer hydroperiod when it does flood. This results in an overall 13% lower proportion of time flooded for the most urban sites.

In testing the response of specific tidal and rainfall constituents to surrounding land coverage, there were mixed results. The amplitudes of two tidal constituents were

most explained by the surrounding urban index, in which a negative logarithmic relationship was modeled (Fig. 8(a)), although there was no relationship between the

combined amplitude of all constituents and surrounding land cover. While these models suggest lower contributions from some tidal constituents in urban mangroves, the contribution from rainfall was not found to be dependent upon degree of urbanization, and instead geomorphology and tidal connectivity were more important (Fig. 8(b)). In this case, partially restricted hydro-geomorphologies responded by increasing water levels five times that of cumulative rainfall. This was significantly greater than the response by open systems at 0.5 times cumulative rainfall (t test; difference: 4.2 cm/cm, $p < 0.05$). There was no relationship between the extent of water level response to rainfall and surrounding urban coverage across sites ($p > 0.5$).

Discussion

There was mixed evidence for a significant influence of urban land cover on flooding dynamics or surface water chemical properties across the mangrove study sites. Both mean depth and proportion of time flooded were best modeled to decrease with surrounding level of urbanization, which was best explained by surrounding vegetation and open water cover (Fig. 7). Yet the models presented in Fig. 7 were no longer significant when MPNMAX was removed from the analysis, suggesting the site may be an unrepresentative outlier. Still, such a result would be expected from a decrease in tidal amplitudes in urban sites, which is consistent with other findings from this study (Fig. 8) as well as indirect findings from another study (Marois and Mitsch 2017). Binomial comparisons of most urban vs. least urban corroborated this by showing lower average depths and flooding frequencies, but longer hydroperiods in the most urban sites (Fig. 7). This implies that urban sites do not flood as often, but when they do, flooding is shallower and more prolonged. This is further corroborated by analyses on

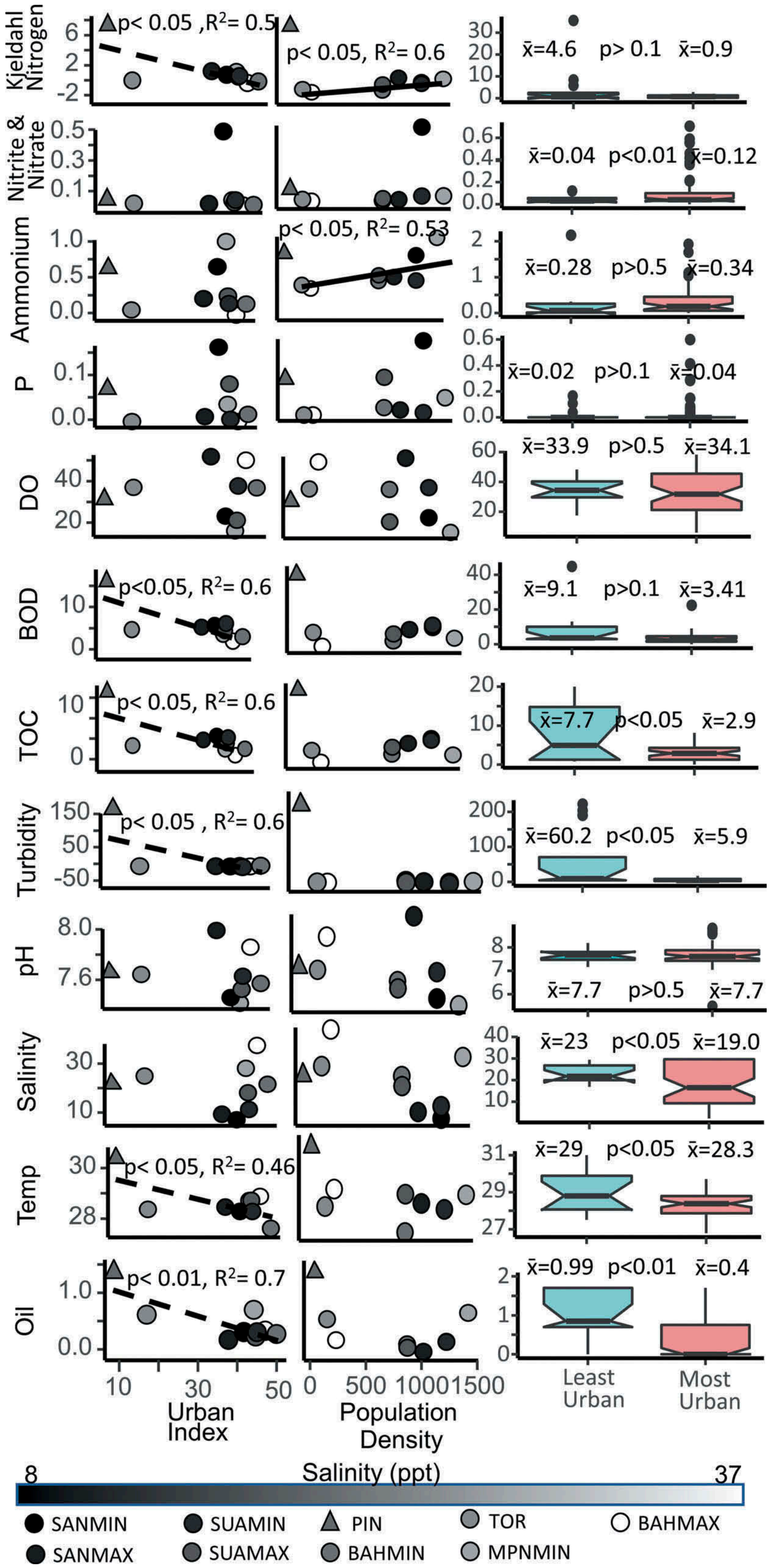

Figure 6. Scatterplots, linear models, and boxplots of surface water chemistry metrics as predicted by surrounding land cover. Lines show statistically significant models ($p < 0.05$). Dashed lines are those with all sites and the solid lines are those without PIN, which was an outlier. Biochemical oxygen demand, nitrogen concentrations, organic carbon, turbidity, oil and grease, and temperature are all predicted to decrease with increasing urbanization. Similar, but sometimes conflicting relationships are evident when comparing the most urban sites with the least urban sites, highlighting the importance of the definition of “urban”. Sites are shaded by salinity to infer on the potential influence of both marine and freshwater.

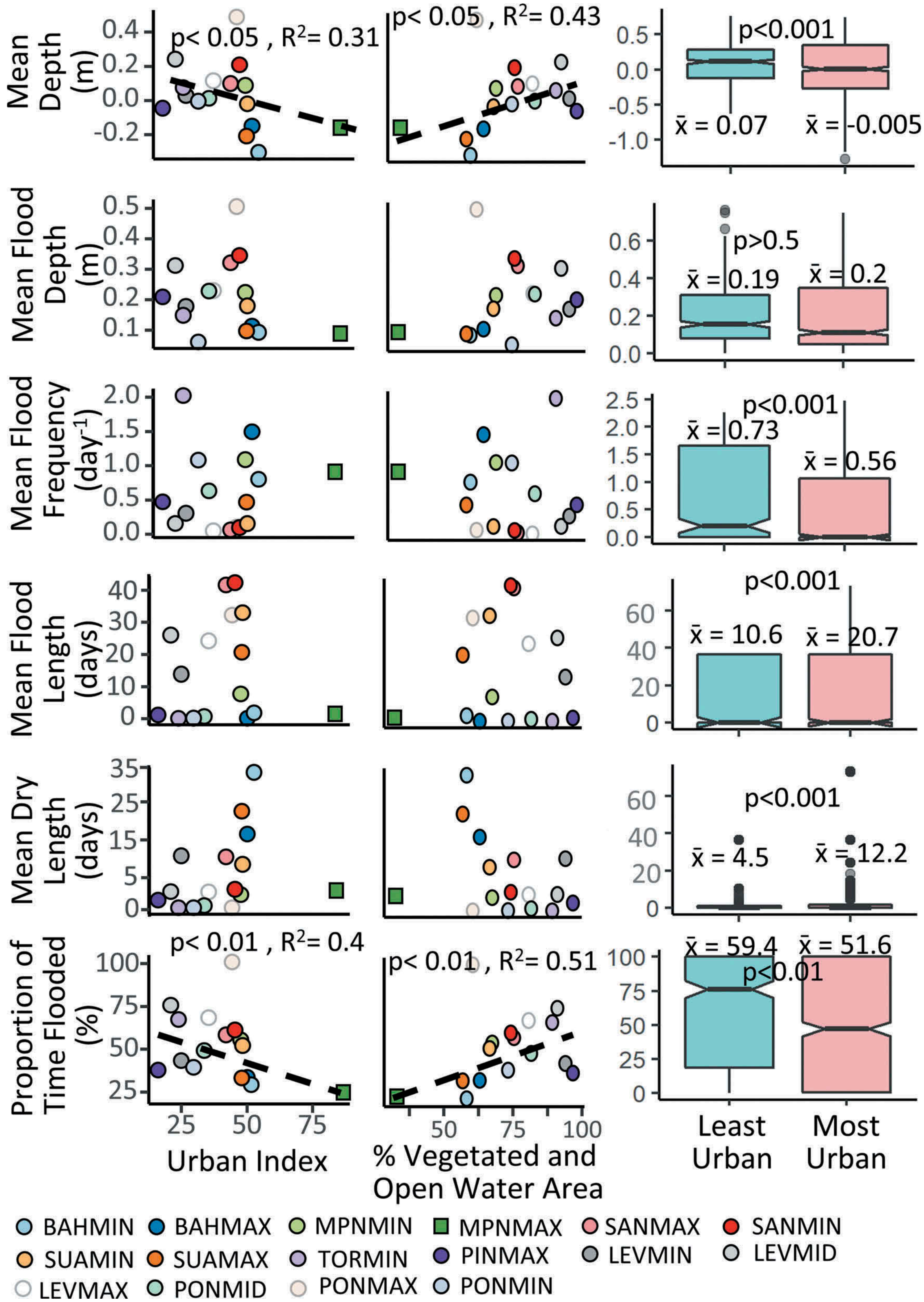

Figure 7. Scatterplots, linear models, and boxplots of flooding metrics as predicted by surrounding land cover. In the scatterplots, lines show statistically significant models ($p < 0.05$). None of the linear models could be repeated without the outlier of MPNMIN. In boxplots, p values are the result of the Student t test and are displayed only when a significant difference resulted between most urban and least urban values. Under this definition, there are significant differences in least urban and most urban mangroves in all flooding metrics except mean flood depth. These results suggest the most urban mangrove are shallower and flood for longer time periods, but overall are flooded less of the time than the least urban mangroves.

individual constituents, in which the amplitudes of the J1 (smaller lunar elliptical diurnal) and 2SM2 (shallow water semidiurnal) constituents were found to decrease as urbanization increased (Fig. 8(a)). The difference in amplitude between the least and most urban sites is around 3 and 1 cm, respectively, for the J1 and 2SM2 constituents, which may be enough to lead to lower average depths in some urban mangrove forests.

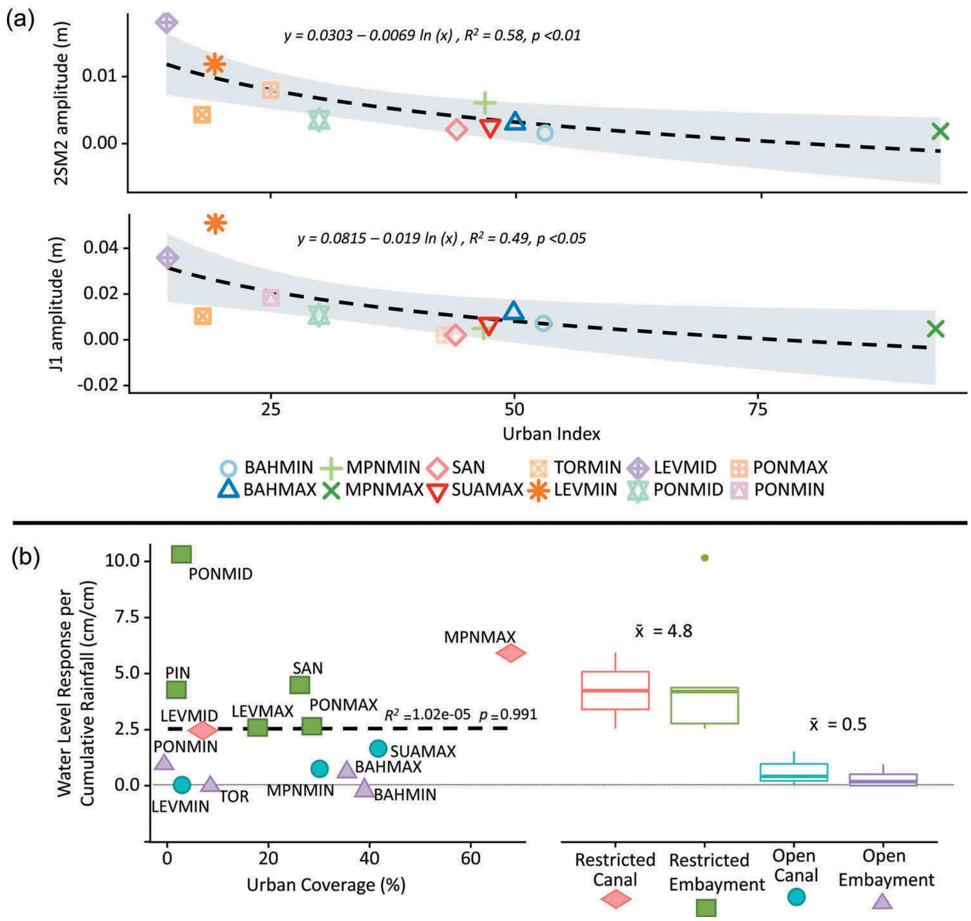

Figure 8. Mixed evidence for the influence of urban land use on mangrove hydrology. (a) The shallow water semidiurnal (2SM2) and the smaller lunar elliptical diurnal (J1) tidal constituents show decreasing amplitude with increasing urban coverage, while (b) there was no evidence for an effect of urbanization on water-level responses to rainfall. Instead, differences in rainfall response were best explained by geomorphology, where partially restricted waterbodies respond more sharply to rainfall than to those that are more open to tidal connections.

The potential explanation for a decrease in tidal amplitudes with urbanization is unclear. It's possible this is in response to urban storm water infrastructure, which may exacerbate rainfall runoff to the point in which it interferes with otherwise normal tidal forcing. This would be consistent with urban hydrology theory (Leopold 1968, Hollis 1975, Lee *et al.* 2006, Dietz and Clausen 2008). But tidal models were constructed in the absence of rainfall within a 4-day period, so all tidal amplitudes should be independent of the influence of precipitation. Further, there was no significant effect of urbanization on the water level responses to rainfall (Fig. 8(b)). Instead, tidal connectivity resulting from geomorphology was found to be more important, where restricted and less connected systems respond more strongly to rainfall than do open and more connected systems (Fig. 8(b)). Urbanization might therefore be influencing tidal components through engineered changes to geomorphology.

Canalization and dredging, for example, are sometimes associated with highly urban landscapes, and are also likely influencing tidal amplitudes through changes in geomorphology. There was some evidence for this in the results. Water levels in the dredged portion of Martín Peña canal (MPNMIN) are nearly identical to those at the mouth of the Río Puerto Nuevo in the San Juan Bay (BAHMAX) (Fig. 3). Farther into the un-dredged and highly constricted Martín Peña (MPNMAX), however, daily water ranges are nearly half that of MPNMIN and the influence of rain on the water level model is five times greater (Figs. 5 and 8 (b)). Thus, it is likely that the dredging of the lower portions of the canal has allowed greater tidal influence and limited response to rainfall. A similar reduction in tidal amplitude and amplification of the importance of rain is seen between SUAMAX and SUAMIN (Fig. 3). These two portions of the Suarez canal are separated by the Baldorioty expressway (PR highway 66) and a network of frontage roads that form a highly engineered constriction, reducing the canal width from roughly 50 to 15 m. In the restricted portion of the canal at SUAMIN and San Jose Lagoon stations (SANMIN and SANMAX), the daily range in water levels is 3.5 times less than that at the tidally connected SUAMAX and the importance of rain in the water level model is nearly six times greater (Figs. 5 and 8(b)). Thus, the constriction of the canal at the highway crossing is likely impeding flood drainage, resulting in greater importance of rainfall and limited tidal connectivity in the upper half of the canal.

With surface water chemical properties, the most significant models could not be repeated without the extreme values of Piñones lagoon (PIN), which is a relatively pristine system with a weak hydrologic connection to the rest of the estuary (Ellis 1976, Lugo *et al.* 2011). Still, biological oxygen demand was modeled to decrease with urbanization, an effect that is opposite of that from previous studies (Mallin *et al.* 2009, Erickson *et al.* 2013), which have shown urban storm water runoff to increase BOD by introducing oxygen demanding substances. The observed trend from Fig. 6 is thus probably spurious as it is unlikely San Juan has the opposite effect on BOD as other urban aquatic systems. Instead, the observed trend is likely due to elevated organic carbon (TOC) and nitrogen (Kjeldahl nitrogen) at Piñones (Sawyer 2003). A multi-variate linear model constructed of these two predictors performed far better than any of the tested land cover metrics (BOD ~TOC + Kjeldahl nitrogen; $R^2 = 0.98$, $p < 0.01$). Apart from BOD, TOC and Kjeldahl nitrogen, Piñones held significantly higher ammonium, turbidity, oil and grease, and temperature, than most other sites, and all trends suggest the opposite of previous studies in which the least urban water bodies hold the lowest nutrient and contaminant concentrations (Mcclelland and Valiela 1998, Mallin *et al.* 2009, Erickson *et al.* 2013). Thus, Piñones being a relatively pristine system, it must be inferred that its anomalous surface water chemistry is explained more by its minimal tidal influence than by urban inputs.

This further demonstrates that hydrology and water chemistry must by studied within the context of geomorphology and tidal connectivity when assessing anthropogenic influences (Kjerfve *et al.* 1999, Adame *et al.* 2010). This is especially important when considering nutrients such as nitrogen and phosphorus, which have repeatedly been associated with urbanization (Groffman *et al.* 2004, Yang 2012, Wigand *et al.* 2014). However, both nitrogen and phosphorus are non-conservative elements that often undergo cyclical biotransformation through various forms, especially in mangrove systems with tidal flushing (Singh *et al.* 2005, Reef *et al.* 2010). Thus, a relative abundance or deficiency in these nutrients may not necessarily be attributable to the urban landscape. As is likely the case in the present study, elevated concentrations of these nutrients may be more influenced by tidal connectivity and geomorphology, among other non-anthropogenic influences.

Other isolated abnormalities could be associated with either urbanization or natural variations in geomorphology and water chemistry. For the former, nitrogen was abnormally high in various forms in some of the water bodies of the San Juan Bay Estuary, providing further evidence for the commonly reported eutrophication of the system (Webb and Gómez-Gómez 1998, Cerco *et al.* 2003). SANMIN, a moderately urban site, also registered higher nitrate and nitrite concentrations than all other water bodies, this time likely due to an excessive amount of wastewater entering the lagoon from the surrounding area through the San Antón creek (Gómez-Gómez and Quiñones 1983). Sewage may also be to blame for high phosphorous concentrations at BAHMIN, which includes the mouth of Malaria canal and the intermittent effluent of sewage (Cruden 2015). Piñones was again singled out from the other water bodies in its flooding dynamics, along with LEVMAX, PONMAX, and PONMID, all of which exhibited significantly greater hydroperiods and maximum flood depths in comparison with the other sites. Again, the likely reasons for these anomalies are mixed. These mangroves are characterized by relatively isolated inland lagoons with little tidal connectivity. As a result, they are more sensitive to precipitation inputs (Rodríguez-Martínez and Soler-López 2014), which induce rapid and prolonged flooding. At PONMAX and LEVMAX, the isolation is likely by design, with both serving as urban storm water retention basins. But Piñones and PONMID are both protected and relatively undisturbed sites with minimal human influence, thus their abnormal hydroperiods are more likely a result of natural forces.

This study used water level models based on months and in some cases years of observations across 16 sites in Puerto Rico. Most of the models explained more than 50% of the observed variations in water levels, and more than half of them explained at least 70% of the variations. The performance criterion of $R^2 > 0.5$ and $E_{RMS} < 0.2$ m allowed for comparisons in which 50% of the water level variability was explained and that the mean error between any two observations was less than 20 cm. These criteria were based on recommendations (Biondi *et al.* 2012, Williams and Esteves 2017), as well on the observation that each criteria emphasizes a particular source of bias and error and that no single criteria provides an ideal measure of model accuracy (Krause *et al.* 2005, Biondi *et al.* 2012). The ideal coefficient of determination (R^2) is widely debated, but for the purposes of this study (comparing influences of water level variability across an urban gradient) it was most important to be able to explain at least 50% of the variability. Although it is likely that additional and unexplained variability from untested variables or inaccurate measurements may change the ultimate results if included in the models, ensuring that at least 50% is accounted for provides confidence that any remaining error is minimal.

One potential source of error is the vertical accuracies of the DEMs (Table 1), which although well within the range of most water levels, are still greater than some of the observed differences in depths between sites. More accurate DEMs that cover such a large area may be available for future studies and could be used to improve upon this analysis. Also, the present study did not include groundwater, evapotranspiration, or fluvial exchanges as there were no direct measurements available. Groundwater inputs are limited to the San Juan Bay and San José Lagoons and have been estimated at around 33 000 $m^3\ d^{-1}$, or %0.8 of the 4.2 $Mm^3\ d^{-1}$ in net tidal exchange from the San Juan Bay (Webb and Gómez-Gómez 1998). Fluvial inputs are likely partially included as precipitation inputs and come only from the Quebrada Blasina, Quebrada San Antón, and the Río Puerto Nuevo at 30 000, 20 000, and 35 000 $m^3\ d^{-1}$, respectively (Webb and Gómez-Gómez 1998). Combined, these exchanges represent roughly 2% of the 4.5 $Mm^3\ d^{-1}$ in net tidal exchanges throughout the estuary. Evaporation is estimated at roughly 2,000 mm yr^{-1} or roughly equivalent to rainfall but spread evenly throughout the year. Thus, while these components are important to quantifying the overall water budget of the study sites, they likely contribute only a small fraction of the overall influence in daily water level fluctuations.

Other improvements can be made by capturing more long-term observations across similarly quantified urban gradients, and by improving the response to rainfall, which was the primary source of unexplained variation. Future studies should consider land cover alongside geomorphology and tidal connectivity, and should attempt to isolate tidal constituents and specific urban components. They should also use varying definitions of urbanization, as it was demonstrated here that binomial classifications of least urban and most urban resulted in significant differences while gradient analyses did not. Doing so will identify potential causal factors and will be an increasingly important task for mangrove management in the Anthropocene.

As urbanization continues to drive ecosystem processes and habitat loss, its influence on mangrove hydrology is not yet well understood. While changes to hydrology and water chemistry are well documented in urban systems, there remains little empirical evidence for specific influences along quantified urban gradients in mangrove systems. This study shows that such evidence remains confounded with other important factors within three watersheds in Puerto Rico. Although there was some evidence for changes in tidal amplitudes and surface water chemical properties in urban sites, there were few consistent trends to tie any variations in water levels or chemistry to surrounding urbanization. Geomorphology and tidal connectivity were found to be important influences, both of which exhibit both natural and anthropogenically induced variations. Future studies must therefore distinguish between specific components of urban landscapes and natural or engineered variations in geomorphology. They may also improve upon the results presented here by using more accurate DEMs and by better capturing the uncertainty in water level responses to rainfall.

Acknowledgements

Research was partly funded by the United States Forest Service International Institute of Tropical Forestry, San Juan, Puerto Rico. Ariel Lugo, Ferdinand Quiñones, and Autumn Oczkowski provided feedback on first drafts.

Disclosure statement

No potential conflict of interest was reported by the author.

ORCID

Benjamin L. Branoff http://orcid.org/0000-0002-8796-2039

References

Acevedo-Figueroa, D., Jiménez, B.D., and Rodriguez-Sierra, C.J., 2006. Trace metals in sediments of two estuarine lagoons from Puerto Rico. *Environmental Pollution*, 141, 336–342. doi:10.1016/j.envpol.2005.08.037

Adame, M.F., Virdis, B., and Lovelock, C.E., 2010. Effect of geomorphological setting and rainfall on nutrient exchange in mangroves during tidal inundation. *Marine and Freshwater Research*, 61, 1197–1206. doi:10.1071/MF10013

Altunkaynak, A., 2007. Forecasting surface water level fluctuations of Lake Van by artificial neural networks. *Water Resources Management*, 21, 399–408. doi:10.1007/s11269-006-9022-6

Bates, D., *et al.*, 2014. *minqa: derivative-free optimization algorithms by quadratic approximation.*

Biondi, D., *et al.*, 2012. Validation of hydrological models: conceptual basis, methodological approaches and a proposal for a code of practice. *Physics and Chemistry of the Earth, Parts A/B/C*, 42, 70–76. doi:10.1016/j.pce.2011.07.037

Bivand, R. and Rundel, C., 2017. *rgeos: interface to geometry engine - open source (GEOS).*

Bivand, R.S., Pebesma, E., and Gomez-Rubio, V., 2013. *Applied spatial data analysis with R*. 2nd ed. New York, NY: Springer.

Bosire, J.O., *et al.*, 2008. Functionality of restored mangroves: a review. *Aquatic Botany*, 89, 251–259. doi:10.1016/j.aquabot.2008.03.010

Bouillon, S., *et al.*, 2007. Importance of intertidal sediment processes and porewater exchange on the water column biogeochemistry in a pristine mangrove creek (Ras Dege, Tanzania). *Biogeosciences Discussions*, 4, 317–348. doi:10.5194/bgd-4-317-2007

Brandeis, T.J., *et al.*, 2014. *San Juan Bay Estuary watershed urban forest inventory*. Asheville, NC: USDA-Forest Service, Southern Research Station, 44, Gen. Tech. Rep. SRS-GTR-190, 190, 1–44.

Branoff, B.L., 2017. Quantifying the influence of urban land-use on mangrove biology and ecology: a meta-analysis. *Global Ecology & Biogeography*, 26, 1339–1356. doi:10.1111/geb.12638

Bunch, B.W., *et al.*, 2000. *Hydrodynamic and water quality model study of San Juan Bay Estuary*. Vicksburg, MS: Engineer Research and Development Center, Army Engineer Waterways Experiment Station.

Cerco, C., *et al.*, 2003. Eutrophication and pathogen abatement in the San Juan Bay Estuary. *Journal of Environmental Engineering*, 129, 318–327. doi:10.1061/(ASCE)0733-9372(2003)129:4(318)

Clough, B.F., Boto, K.G., and Attiwill, P.M., 1983. Mangroves and sewage: a re-evaluation. *In*: H. Teas, ed. *Biology and ecology of mangroves*. Netherlands: Springer Netherlands, 151–161.

Colonnello, G. and Medina, E., 1998. Vegetation changes induced by dam construction in a tropical estuary: the case of the Mánamo river, Orinoco Delta (Venezuela). *Plant Ecology*, 139, 145–154. doi:10.1023/A:1009785118019

Cruden, J.C., 2015. *USA v. PRASA and The Commonwealth of Puerto Rico* [online]. D. Puerto Rico, consent decree No. 3:15-cv-02283. Available from: https://echo.epa.gov/enforcement-case-report?id=02-2011-0007

Dawson, C.W. and Wilby, R., 1998. An artificial neural network approach to rainfall-runoff modelling. *Hydrological Sciences Journal*, 43, 47–66. doi:10.1080/02626669809492102

Dietz, M.E. and Clausen, J.C., 2008. Stormwater runoff and export changes with development in a traditional and low impact subdivision. *Journal of Environmental Management*, 87, 560–566. doi:10.1016/j.jenvman.2007.03.026

Ellis, S.R., 1976. *History of dredging and filling of lagoons in the San Juan area, Puerto Rico*. US Geological Survey, Water-Resources Investigations, 38 (76).

Ellison, A.M. and Farnsworth, E.J., 1996. Anthropogenic disturbance of Caribbean Mangrove Ecosystems: past impacts, present trends, and future predictions. *Biotropica*, 28, 549–565. doi:10.2307/2389096

Erickson, A.J., Weiss, P.T., and Gulliver, J.S., 2013. Impacts and composition of urban stormwater. *In*: *Optimizing stormwater treatment practices*. New York, NY: Springer, 11–22.

Ewel, K., Twilley, R., and Ong, J.I.N., 1998. Different kinds of mangrove forests provide different goods and services. *Global Ecology & Biogeography Letters*, 7, 83–94. doi:10.2307/2997700

Faulkner, S., 2004. Urbanization impacts on the structure and function of forested wetlands. *Urban Ecosystems*, 7, 89–106. doi:10.1023/B:UECO.0000036269.56249.66

Feller, I.C., *et al.*, 2003. Nitrogen vs. phosphorus limitation across an ecotonal gradient in a mangrove forest. *Biogeochemistry*, 62, 145–175. doi:10.1023/A:1021166010892

Gleeson, J., *et al.*, 2013. Groundwater–surface water exchange in a mangrove tidal creek: evidence from natural geochemical tracers and implications for nutrient budgets. *Marine Chemistry*, 156, 27–37. doi:10.1016/j.marchem.2013.02.001

Gómez-Gómez, F. and Quiñones, F., 1983. *Hydrologic charactersitics of lagoons at San Juan, Puerto Rico, during an October 1974 tidal cycle*. US Geological Survey, Water-Resources Investigations, 38 (75).

Groffman, P.M., *et al.*, 2004. Nitrogen fluxes and retention in urban watershed ecosystems. *Ecosystems*, 7, 393–403. doi:10.1007/s10021-003-0039-x

Grömping, U., 2006. Relative importance for linear regression in R: the package relaimpo. *Journal of Statistical Software*, 17, 1–27. doi:10.18637/jss.v017.i01

Hamilton, S., and Casey, D, 2016. Creation of a high spatiotemporal resolution global database of continuous mangrove forest cover for the 21st century (CGMFC-21). *Global Ecology & Biogeography*, 25.6, 729–738.
Hijmans, R., 2016. *raster: geographic data analysis and modeling*. R package version 2.5-8.
Hollis, G.E., 1975. The effect of urbanization on floods of different recurrence interval. *Water Resources Research*, 11, 431–435. doi:10.1029/WR011i003p00431
House, M.A., *et al*., 1993. Urban drainage–impacts on receiving water quality. *Water Science and Technology*, 27, 117–158. doi:10.2166/wst.1993.0293
Kjerfve, B., *et al*., 1999. Hydrological and hydrogeochemical variations in mangrove ecosystems. *In*: A. Yanez-Arancibia and A. Lara-Dominquez, eds. *Mangrove ecosystems in tropical America: structure, function and management*. INECOL: Mexico; IUCN/ORMA: Costa Rica; NOAA/NMFS: Beaufort, NC, USA, 71–81.
Koutsoyiannis, D. and Onof, C., 2001. Rainfall disaggregation using adjusting procedures on a Poisson cluster model. *Journal of Hydrology*, 246, 109–122.
Krause, P., Boyle, D.P., and Bäse, F., 2005. Comparison of different efficiency criteria for hydrological model assessment. *Advances in Geosciences*, 5, 89–97. doi:10.5194/adgeo-5-89-2005
Krauss, K.W., *et al*., 2006. Evaluating the relative contributions of hydroperiod and soil fertility on growth of south Florida mangroves. *Hydrobiologia*, 569, 311–324.
Lee, S.Y., *et al*., 2006. Impact of urbanization on coastal wetland structure and function. *Austral Ecology*, 31, 149–163. doi:10.1111/j.1442-9993.2006.01581.x
Lee, S.Y., *et al*., 2014. Ecological role and services of tropical mangrove ecosystems: a reassessment. *Global Ecology and Biogeography*, 23, 726–743. doi:10.1111/geb.12155
Leopold, L.B., 1968. *Hydrology for urban land planning: a guidebook on the hydrologic effects of urban land use*. US Department of the Interior, Geological Survey.
Lewis, R.R., 2005. Ecological engineering for successful management and restoration of mangrove forests. *Ecological Engineering*, 24, 403–418. doi:10.1016/j.ecoleng.2004.10.003
Lindeman, R.H., 1980. *Introduction to bivariate and multivariate analysis*. Glenview, IL: Scott Foresman.
Lovelock, C.E., *et al*., 2009. Nutrient enrichment increases mortality of mangroves. *PloS One*, 4, e5600. doi:10.1371/journal.pone.0005600
Lugo, A.E. and Medina, E., 2014. *Mangrove forests. Encyclopedia of natural resources*. New York, NY: Taylor & Francis, 343–352.
Lugo, A.E., Ramos, O., and Rodriguez, C., 2011. *The Río Piedras watershed and its surrounding environment*. US Department of Agriculture, Forest Service, International Institute of Tropical Forestry, 46, FS-980, 980.
Lugo, A.E. and Snedaker, S.C., 1974. The ecology of mangroves. *Annual Review of Ecology and Systematics*, 5, 39–64. doi:10.1146/annurev.es.05.110174.000351
Mallin, M.A., Johnson, V.L., and Ensign, S.H., 2009. Comparative impacts of stormwater runoff on water quality of an urban, a suburban, and a rural stream. *Environmental Monitoring and Assessment*, 159, 475–491. doi:10.1007/s10661-008-0644-4
Mandura, A.S., 1997. A mangrove stand under sewage pollution stress: Red Sea. *Mangroves and Salt Marshes*, 1, 255–262. doi:10.1023/A:1009927605517
Marois, D.E. and Mitsch, W.J., 2017. A mangrove creek restoration plan utilizing hydraulic modeling. *Ecological Engineering*, 108, 537–546. doi:10.1016/j.ecoleng.2017.06.063
Martinuzzi, S., *et al*., 2009. Conversion and recovery of Puerto Rican mangroves: 200 years of change. *Forest Ecology and Management*, 257, 75–84. doi:10.1016/j.foreco.2008.08.037
Mcclelland, J.W. and Valiela, I., 1998. Linking nitrogen in estuarine producers to land-derived sources. *Limnology and Oceanography*, 43, 577–585. doi:10.4319/lo.1998.43.4.0577
Mcmahon, G. and Cuffney, T.F., 2000. Quantifying urban intensity in crainage basins for assessing stream ecological conditions. *Journal of the American Water Resources Association*, 36, 1247–1261. doi:10.1111/j.1752-1688.2000.tb05724.x
Medina, E., 1999. Mangrove physiology: the challenge of salt, heat, and light stress under recurrent flooding. *In*: A. Yánez-Arancibia and A. L. Lara-Domínguez, eds. *Ecosistemas de manglar en América tropical*. Xalapa, México: Instituto de Ecología, AC; Costa Rica: UICN/ORMA; Silver Spring MD: NOAA/NMFS, 109–126.
NOAA (National Oceanic and Atmospheric Administration), 2017a. *2015 NOAA NGS Topobathy Lidar DEM: Puerto Rico*. National Centers for Environmental Information, NESDIS, NOAA, US Department of Commerce.
NOAA (National Oceanic and Atmospheric Administration), 2017b. *San Juan, Puerto Rico 1/9 arc-second PRVD Coastal Digital Elevation Model*. National Centers for Environmental Information, NESDIS, NOAA, US Department of Commerce.
NOAA BP (National Oceanic and Atmospheric Administration Biogeography Program), 2011. *Benthic habitats of Puerto Rico*. Charleston, SC: NOAA Coastal Services Center.
Office for Coastal Management, 2020. *C-CAP Land Cover, Puerto Rico, 2010 from 2010-06-15 to 2018-08-15*. INFORMATION, N. N. C. F. E. ed.
Pagliosa, P.R., *et al*., 2006. Urbanization impact on subtropical estuaries: a comparative study of water properties in urban areas and in protected areas. *Journal of Coastal Research*, (S139), 731–735.
Powell, M.J.D., 2009. *The BOBYQA algorithm for bound constrained optimization without derivatives*. Cambridge: University of Cambridge, Cambridge NA Report NA2009/06, 26–46.
Reef, R., Feller, I.C., and Lovelock, C.E., 2010. Nutrition of mangroves. *Tree Physiology*, 30, 1148–1160. doi:10.1093/treephys/tpq048
Rodríguez-Martínez, J. and Soler-López, L.R., 2014. *Hydrogeology and hydrology of the Punta Cabullones wetland area, Ponce, southern Puerto Rico, 2007–08*. US Geological Survey, 2328-032.
Sakho, I., *et al*., 2011. The influence of natural and anthropogenic factors on mangrove dynamics over 60 years: the Somone Estuary, Senegal. *Estuarine, Coastal and Shelf Science*, 94, 93–101. doi:10.1016/j.ecss.2011.05.032
Sawyer, C.N., 2003. *Chemistry for environmental engineering and science*. New York, NY: McGraw-Hill Education.
Seguinot Barbosa, J., 1996. La ecologia urbana de San Juan. Una interpretación geográfica-social. *Anales de Geografía de la Universidad Complutense*, 16, 161–184.
Seguinot-Barbosa, J., 1983. *Coastal modification and land transformation in the San Juan Bay Area: Puerto Rico*. (Doctor of Philosophy). Louisiana State Univeristy.
Sherman, R.E., Fahey, T.J., and Howarth, R.W., 1998. Soil-plant interactions in a neotropical mangrove forest: iron, phosphorus and sulfur dynamics. *Oecologia*, 115, 553–563. doi:10.1007/s004420050553
Singh, G., Ramanathan, A.L., and Prasad, M.B.K., 2005. Nutrient cycling in mangrove ecosystem: a brief overview. *International Journal of Ecology and Environmental Sciences*, 30, 231–244.
Stephenson, A.G., 2016. *Harmonic analysis of tides using TideHarmonics* [online]. Available from: https://CRAN.R-project.org/package=TideHarmonics
Sutula, M., *et al*., 2001. Hydrological and nutrient budgets of freshwater and estuarine wetlands of Taylor Slough in Southern Everglades, Florida (USA). *Biogeochemistry*, 56, 287–310. doi:10.1023/A:1013121111153
Temple Lang, D., 2014. *RJSONIO: serialize R objects to JSON, JavaScript Object Notation*. R package version 1.3-0.
Tian-Hong, L., Peng, H., and Zhi-Jie, Z., 2008. Impact analysis of coastal engineering projects on mangrove wetland area change with remote sensing. *China Ocean Engineering*, 22, 347–358.
Toth, E., Brath, A., and Montanari, A., 2000. Comparison of short-term rainfall prediction models for real-time flood forecasting. *Journal of Hydrology*, 239, 132–147. doi:10.1016/S0022-1694(00)00344-9
Turner, R., 2017. *deldir: Delaunay triangulation and Dirichlet (Voronoi) Tessellation*.
Twilley, R.R. and Chen, R., 1998. A water budget and hydrology model of a basin mangrove forest in Rookery Bay, Florida. *Marine and Freshwater Research*, 49, 309–323. doi:10.1071/MF97220
Ulrich, J., 2017. *TTR: technical trading rules*. Version 0.23-6 ed.
USACE (US Army Corps of Engineers), 1987. *A study to determine the feasability of providing flood control on the rio de la plata in Toa Baja - Dorado Area, Puerto Rico. ed.* Jacksonville.

USACE (US Army Corps of Engineers), 2015. *Final environmental impact statement Cano Martín Pena Ecosystem Restoration Project San Juan*. Puerto Rico.

USCB (US Census Bureau), 2017a. *2010 Tiger/Line Shapefiles of total population at census block level*. Suitland, MD: USCB.

USCB (US Census Bureau), 2017b. *2010 Tiger/Line Shapefiles of roads*. Suitland, MD: USCB.

Villate, F., *et al*., 2013. Dissolved oxygen in the rehabilitation phase of an estuary: influence of sewage pollution abatement and hydro-climatic factors. *Marine Pollution Bulletin*, 70, 234–246. doi:10.1016/j.marpolbul.2013.03.010

Webb, R.M.T. and Gómez-Gómez, F., 1998. *Synoptic survey of water quality and bottom sediments, San Juan Bay estuary system, Puerto Rico, December 1994-July 1995*. US Geological Survey.

Wickham, H., 2009. *ggplot2: elegant graphics for data analysis*.

Wigand, C., *et al*., 2014. Below the disappearing marshes of an urban estuary: historic nitrogen trends and soil structure. *Ecological Applications*, 24, 633–649. doi:10.1890/13-0594.1

Williams, J.J. and Esteves, L.S., 2017. Guidance on setup, calibration, and validation of hydrodynamic, wave, and sediment models for shelf seas and estuaries. *Advances in Civil Engineering*, 2017. Article ID 5251902. doi:10.1155/2017/5251902

Wolanski, E., Mazda, Y., and Ridd, P., 1993. Mangrove hydrodynamics. *In*: A. Robertson and D. Alongi, eds. *Tropical Mangrove Ecosystems*. Washington, DC: American Geophyscial Union, 43–62.

Wong, Y.S., Tam, N.F.Y., and Lan, C.Y., 1997. Mangrove wetlands as wastewater treatment facility: a field trial. *In*: Y.-S. Wong and N.-Y. Tam, eds. *Hydrobiologia*. Belgium: Springer Netherlands, 49–59.

Yan, J., *et al*., 2011. R: a language and environment for statistical computing. *R Foundation for Statistical Computing*, 1, 409.

Yang, X., 2012. An assessment of landscape characteristics affecting estuarine nitrogen loading in an urban watershed. *Journal of Environmental Management*, 94, 50–60. doi:10.1016/j.jenvman.2011.07.025

Zeilis, A. and Grothendieck, G., 2005. zoo: S3 infrastructure for regular and irregular time series. *Journal of Statistical Software*, 14, 1–27.